Cell Reports, Volume *31*

Supplemental Information

Variation of Human Neural Stem Cells Generating Organizer States *In Vitro* before Committing to Cortical Excitatory or Inhibitory Neuronal Fates

Nicola Micali, Suel-Kee Kim, Marcelo Diaz-Bustamante, Genevieve Stein-O'Brien, Seungmae Seo, Joo-Heon Shin, Brian G. Rash, Shaojie Ma, Yanhong Wang, Nicolas A. Olivares, Jon I. Arellano, Kristen R. Maynard, Elana J. Fertig, Alan J. Cross, Roland W. Bürli, Nicholas J. Brandon, Daniel R. Weinberger, Joshua G. Chenoweth, Daniel J. Hoeppner, Nenad Sestan, Pasko Rakic, Carlo Colantuoni, and Ronald D. McKay

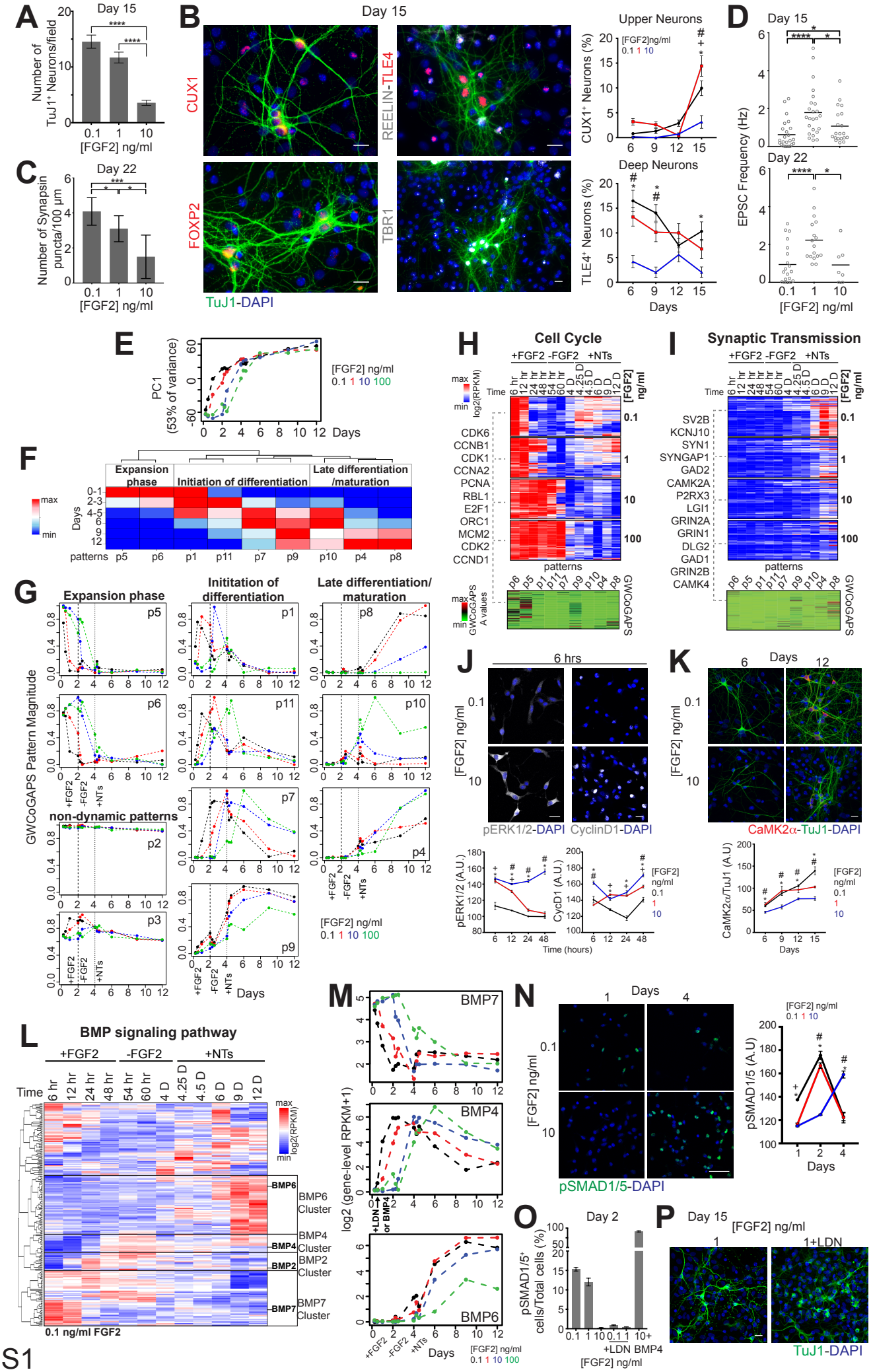
A
Day 15
Number of TuJ1+ Neurons/field
[FGF2] ng/ml
B
Day 15
CUX1
REELIN-TLE4
FOXP2
TBR1
TuJ1-DAPI
Upper Neurons
CUX1+ Neurons (%)
Deep Neurons
TLE4+ Neurons (%)
Days
C
Day 22
Number of Synapsin puncta/100 µm
D
Day 15
Day 22
EPSC Frequency (Hz)
E
PC1 (53% of variance)
Days
F
Expansion phase
Initiation of differentiation
Late differentiation /maturation
patterns
G
Expansion phase
Initiation of differentiation
Late differentiation/ maturation
non-dynamic patterns
GWCoGAPS Pattern Magnitude
H
Cell Cycle
I
Synaptic Transmission
J
6 hrs
pERK1/2-DAPI
CyclinD1-DAPI
Time (hours)
K
Days
CaMK2α-TuJ1-DAPI
L
BMP signaling pathway
BMP6 Cluster
BMP4 Cluster
BMP2 Cluster
BMP7 Cluster
M
BMP7
BMP4
BMP6
N
pSMAD1/5-DAPI
O
Day 2
pSMAD1/5+ cells/Total cells (%)
P
Day 15
1
1+LDN
TuJ1-DAPI

Figure S1

Figure S1. Transcriptional dynamics and BMP signaling across mouse *in vitro* neurogenesis. Related to Figure 1. Cortical neuron type and maturation regulated by early FGF2 signaling in mouse NSCs (**A-D**). (**A**) Mean number of TuJ1$^+$ neurons/field, from 4 independent DIV 15 cultures, t-test. (**B**) (Left) Immuno-fluorescence images of TuJ1$^+$ neurons over rat astrocytes, expressing CUX1, REELIN, TLE4, FOXP2, or TBR1 at DIV 15. Scale Bars: 20 µm. (Right) Percentage of TuJ1$^+$ neurons expressing TLE4 or CUX1. ANOVA comparing FGF2 doses. Significance ($p<0.05$) is represented as *: 0.1 vs 10; #: 1 vs 10; +: 0.1 vs 1. **(C)** Counts of individually segmented Synapsin1 puncta per 100 µm of neurite length also individually segmented in DIV 22 TuJ1$^+$ neurons. Mean + St.Dev., t-test; n > 5 fields per measurement. **(D)** Mean frequency of Excitatory Post Synaptic Currents (EPSCs) in DIV 15 and 22 neurons derived from 0.1, 1 or 10 ng/ml FGF2 condition. t-test.
Transcriptional dynamics of *in vitro* mouse NSC differentiation (**E-G**). (**E**) PCA of gene-level RNA-seq data from 6 hours to 12 days of differentiation. NSCs were exposed to varying FGF2 doses and differentiated. (**F**) Hierarchical clustering of patterns defined by GWCoGAPS. (**G**) The 11 patterns defined by GWCoGAPS NMF algorithm across FGF2 doses and differentiation time, organized into three major groups, as defined by hierarchical clustering analysis in (F).
Cell cycle activity of NSCs related to neuronal differentiation (**H-K**). (**H**) (Top) Expression levels of selected GO "cell cycle" genes. Well know cell cycle genes are indicated on the left of the heat map. (Bottom) Gene weights for the same genes in each GWCoGAPS pattern. (**I**) (Top) Expression levels of selected GO "synaptic transmission" genes. Well know synaptic genes are indicated on the left of the heat map. (Bottom) Gene weights for the same genes in each GWCoGAPS pattern. Color key as in H. (**J**) (Top) Immuno-fluorescence images of pERK and Cyclin D1 expression in NSCs, 6 hours after plating. Phosphorylation of MAPK/ERK and expression of Cyclin D1 were sensitive to FGF2 dose. Scale bars: 20 µm. (Bottom) Mean signal intensity of pERK and Cyclin D1 (CycD1) within individually segmented cells from high-throughput image analysis, across FGF2 doses and time, from 6 to 48 hours, ± St.Dev. ANOVA comparing FGF2 doses. Significance ($p<0.05$) is represented as *: 0.1 versus 10; #: 1 versus 10; +: 0.1 versus 1. (**K**) Synaptic maturation genes increased when NSCs abruptly left the cell cycle in low FGF2. (Top) Immuno-fluorescence images of CaMK2α expression in TuJ1$^+$ neurons over rat astrocytes, at DIV 6 and 12. Scale bar: 20 µm. (Bottom) Mean signal intensity of CaMK2α normalized over TuJ1 intensity, across FGF2 doses and time, ± St.Dev. ANOVA comparing FGF2 doses. Significance ($p<0.05$) is represented as *: 0.1 versus 10; #: 1 versus 10; +: 0.1 versus 1 FGF2. In low FGF2, NSCs down-regulate cell cycle genes and traverse later steps of neuron differentiation more efficiently than in high FGF2.
Endogenous BMP signaling dynamics across mouse *in vitro* neurogenesis (**L-P**). (**L**) Expression of genes in the "BMP receptor signaling" gene set from NCI http://www.pathwaycommons.org/pc/record2.do?id=517222 (Gene Set: Entrez Gene IDs). In boxes, gene clusters defined by hierarchical clustering including different BMP ligands. 0.1 ng/ml FGF2 is shown. Genes correlated with BMP7, BMP4, BMP6 clusters were summarized in Figure 1. (**M**) Expression of BMP7, BMP4 and BMP6 from RNA-seq data. BMP signaling modulation with LDN and BMP4 is illustrated for BMP4 plot. (**N**) (Left) Immuno-fluorescence images of pSMAD1/5 in NSCs. Scale bar: 50 µm. (Right) Mean signal intensity of pSMAD1/5 within individually nuclear segmented cells from high-throughput image analysis, at the indicated days after NSC plating, ± St.Dev. ANOVA comparing FGF2 doses. Significance ($p<0.05$) is represented as *: 0.1 vs 10; #: 1 vs 10; +: 0.1 vs 1. (**O**) Proportion of individually segmented pSMAD1/5$^+$ NSCs from high-throughput image analysis, relative to total cell number at DIV 2 for 0.1, 1 or 10 ng/ml FGF2; 0.1 and 1 ng/ml FGF2 plus LDN193189 (100 nM); 10 ng/ml FGF2 plus BMP4 (10 ng/ml); LDN or BMP4 were added 12 hours after plating. Mean values + St.Dev. (**P**) Immuno-fluorescence images of DIV 15 TuJ1$^+$ neurons over rat astrocytes derived from 1 ng/ml FGF2 condition plus or minus LDN (100 nM), added 12 hours after plating and withdrawn with FGF2 at DIV 2. Scale bar: 20 µm. The image shows well differentiated neurons with defined dendrites in control vs compromised TuJ1$^+$ cells with aberrant neuron morphology derived from NSCs exposed to LDN.

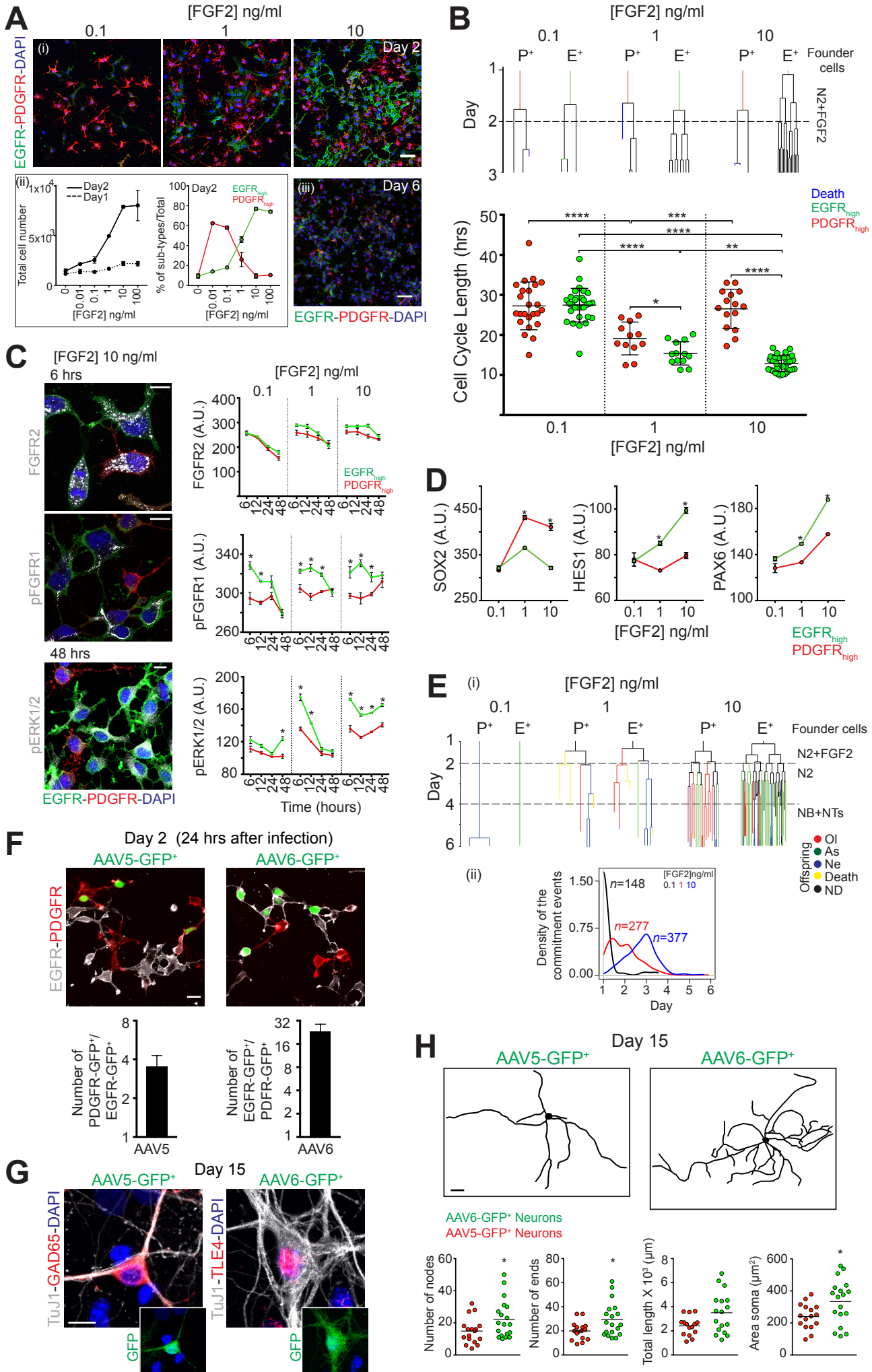
A
[FGF2] ng/ml
0.1
1
10
EGFR-PDGFR-DAPI
(i)
Day 2
(ii)
Day2
Day1
Total cell number
% of sub-types/Total
EGFR high
PDGFR high
[FGF2] ng/ml
(iii)
Day 6
EGFR-PDGFR-DAPI
B
[FGF2] ng/ml
Day
P+
E+
Founder cells
N2+FGF2
Death
EGFR high
PDGFR high
Cell Cycle Length (hrs)
[FGF2] ng/ml
C
[FGF2] 10 ng/ml
6 hrs
48 hrs
FGFR2
pFGFR1
pERK1/2
EGFR-PDGFR-DAPI
[FGF2] ng/ml
FGFR2 (A.U.)
pFGFR1 (A.U.)
pERK1/2 (A.U.)
Time (hours)
D
SOX2 (A.U.)
HES1 (A.U.)
PAX6 (A.U.)
[FGF2] ng/ml
EGFR high
PDGFR high
E
(i)
[FGF2] ng/ml
Founder cells
N2+FGF2
N2
NB+NTs
Day
Offspring
Ol
As
Ne
Death
ND
(ii)
Density of the commitment events
n=148
n=277
n=377
[FGF2]ng/ml
0.1 1 10
Day
F
Day 2 (24 hrs after infection)
AAV5-GFP+
AAV6-GFP+
EGFR-PDGFR
Number of PDGFR-GFP+/ EGFR-GFP+
Number of EGFR-GFP+/ PDFR-GFP+
AAV5
AAV6
G
Day 15
AAV5-GFP+
AAV6-GFP+
TuJ1-GAD65-DAPI
TuJ1-TLE4-DAPI
GFP
H
Day 15
AAV5-GFP+
AAV6-GFP+
AAV6-GFP+ Neurons
AAV5-GFP+ Neurons
Number of nodes
Number of ends
Total length X 10³ (µm)
Area soma (µm²)

Figure S2

Figure S2. Mouse cortical NSC subtypes show selective BMP signaling activation and distinct fate bias. Related to Figure 2. Selective response to FGF2 signaling by mouse NSC subtypes (**A-D**). (**A**) (i) Immuno-fluorescence images of PDGFRα and EGFR expression in NSCs at day 2 of FGF2 modulation. Scale bar: 50 µm. (ii) (Left) Proliferation curves of NSCs at DIV 1 and 2 in different FGF2 doses. (Right) Proportion of PDGFRα_{high} and EGFR$_{high}$ cells at DIV 2, from the high-throughput density plot shown in Figure 2A. (iii) Images of PDGFRα and EGFR expression in differentiated cells at DIV 6, after exposure to 10 ng/ml FGF2 in the first 2 days. Scale bar: 100 µm. (**B**) (Top) Lineage dendrograms from 2 days time-lapse recording. Colored segments reflect fluorescence signal at time T=0 for PDGFRα_{high} (red) vs EGFR$_{high}$ (green) founder cells. Recording started at DIV 1, T=0. Death fated cells are indicated in blue. (Bottom) Duration of the first inter-mitosis intervals. Mean length ± St.Dev. t-test. (**C**) (Left) Immuno-fluorescence images of EGFR$_{high}$ and PDGFRα_{high} NSCs expressing FGFR2 or pFGFR at 6 hours, or pERK at 48 hours after plating in 10 ng/ml FGF2. Scale bars: 10µm. (Right) Mean signal intensity of FGFR2, pFGFR and pERK level within individually segmented EGFR$_{high}$ and PDGFRα_{high} cells, from high-throughput image analysis, ± St.Dev. t-test. Significance is indicated as * for every $p < 0.05$. (**D**) Mean signal intensity of SOX2, HES1 and PAX6 expression within individually nuclear segmented EGFR$_{high}$ and PDGFRα_{high} cells, from high-throughput image analysis, ± St.Dev. t-test. Significance is indicated as * for every $p < 0.05$.
Distinct fate bias of EGFR$_{high}$ and PDGFRα_{high} NSCs (**E-H**). (**E**) (i) Representative lineage dendrograms from 5 days time-lapse recordings of PDGFRα_{high} and EGFR$_{high}$ founder NSCs cultured with different doses of FGF2 and identified at DIV 1, to derivative neurons, oligodendrocytes or astrocytes identified by expression of TuJ1, O4 and GFAP at DIV 6 (see Video S1-3). Recording started at DIV 1, T=0 . Ol: oligodendrocyte; As: astrocyte; Ne: neuron; Death: apoptotic cell; ND: not determined. (ii) Commitment events density plot derived from all the cells traced, independently of the receptor expression. The plot shows that faster cell cycle exit correlates with early fate commitment of the NSCs. Number of total cells traced per condition: 1106 in 10 ng/ml FGF2; 646 in 1 ng/ml FGF2; 202 in 0.1 ng/ml FGF2. *n*= number of terminal offspring cells for each lineage analysis. (**F**) (Top) Immuno-fluorescence images of PDGFRα_{high} and EGFR$_{high}$ NSCs at DIV 2, 24 hours after infection with AAV5-GFP or AAV6-GFP. Scale bar: 20 µm. (Bottom) Preferential tropism of AAV5 for PDGFRa and AAV6 for EGFR expressing cells determined respectively as rate of PDGFRα_{high} / EGFR$_{high}$ cells infected by AAV5 or EGFR$_{high}$ / PDGFRα_{high} cells infected by AAV6, 24 hours after infection. (**G**) Representative immuno-fluorescence images of AAV5-GFP$^+$ and AAV6-GFP$^+$ DIV 15 TuJ1$^+$ neurons, expressing GAD65 or TLE4. Scale bar: 10 µm. (**H**) (Top) Morphological analysis of AAV5-GFP$^+$ and AAV6-GFP$^+$ DIV 15 neurons. Scale bar: 20 µm. (Bottom) Mean value (lines) of the indicated parameters analyzed in individual neurons (dots). t-test.

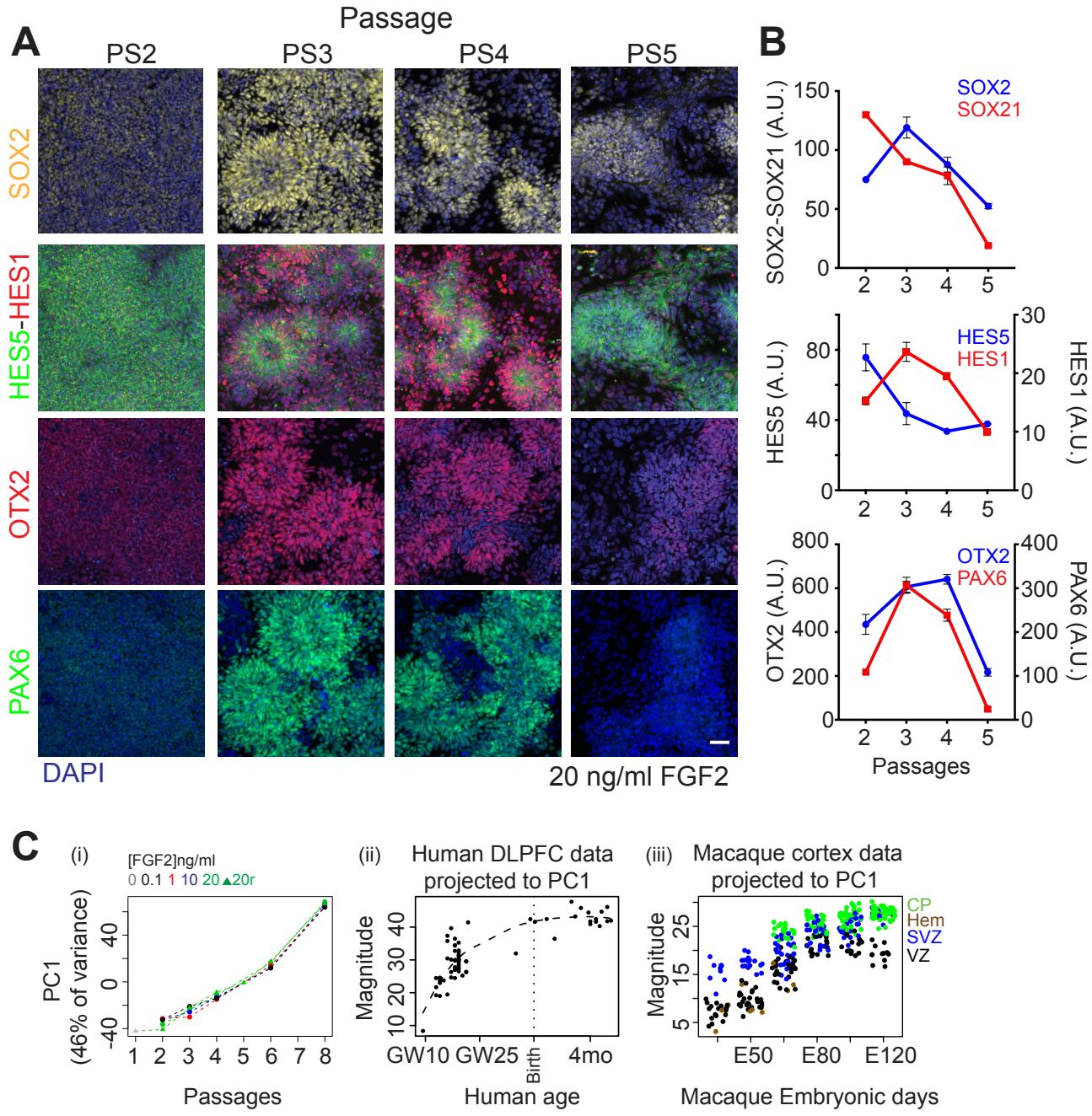
A
Passage
PS2
PS3
PS4
PS5
SOX2
HES5-HES1
OTX2
PAX6
DAPI
20 ng/ml FGF2
B
SOX2
SOX21
SOX2-SOX21 (A.U.)
HES5
HES1
HES5 (A.U.)
HES1 (A.U.)
OTX2
PAX6
OTX2 (A.U.)
PAX6 (A.U.)
Passages
C
(i)
[FGF2]ng/ml
0 0.1 1 10 20 20r
PC1 (46% of variance)
Passages
(ii)
Human DLPFC data projected to PC1
Magnitude
GW10 GW25 Birth 4mo
Human age
(iii)
Macaque cortex data projected to PC1
CP
Hem
SVZ
VZ
Magnitude
E50 E80 E120
Macaque Embryonic days
D
GWCoGAPS Pattern Magnitude
p1
p2
p3
p4
p5
p6
p7
p8
p9
p10
p11
p12
p13
p14
p15
p16
p17
p18
p19
p20
p21
p22
p23
p24
Passages
[FGF2]ng/ml
0 0.1 1 10 20 20r

Figure S3

Figure S3. Cortical excitatory neuron fate bias at a specific passage of human NSCs. Related to Figure 3. Dorsal telencephalic NSCs generated from human PSCs *in vitro*. (**A**) Immuno-fluorescence of the fate regulators SOX2, HES5 and HES1, OTX2, PAX6 expression from PS1 to PS5, 6 days after passage. Scale bar: 50 μm. (**B**) Mean fluorescence intensity in individual segmented cells from high-throughput image analysis, for the indicated markers at every passage. ± St.Dev. (**C**) (i) PCA of gene-level RNAseq data from hNSCs. FGF2 doses are indicated. 0 ng/ml FGF2 refers to PS1; 20r refers to PS2-PS8 sample replicates for 20 ng/ml FGF2. (ii) Projections of human DLPFC RNAseq data (Jaffe et al., 2018) into PC1; (iii) Projection of laser micro-dissected macaque cortex microarray data (Bakken et al., 2016) into PC1. PC1 describes a progressive change *in vitro* that parallels the *in vivo* development of the cortex, as CP emerges from the germinal VZ and SVZ. CP: cortical plate; Hem: cortical Hem; SVZ: subventricular zone; VZ: ventricular zone. (**D**) 24 patterns defined by GWCoGAPS. FGF2 doses are indicated. 0 ng/ml FGF2 refers to PS1; 20r refers to PS2-PS8 sample replicates for 20 ng/ml FGF2.

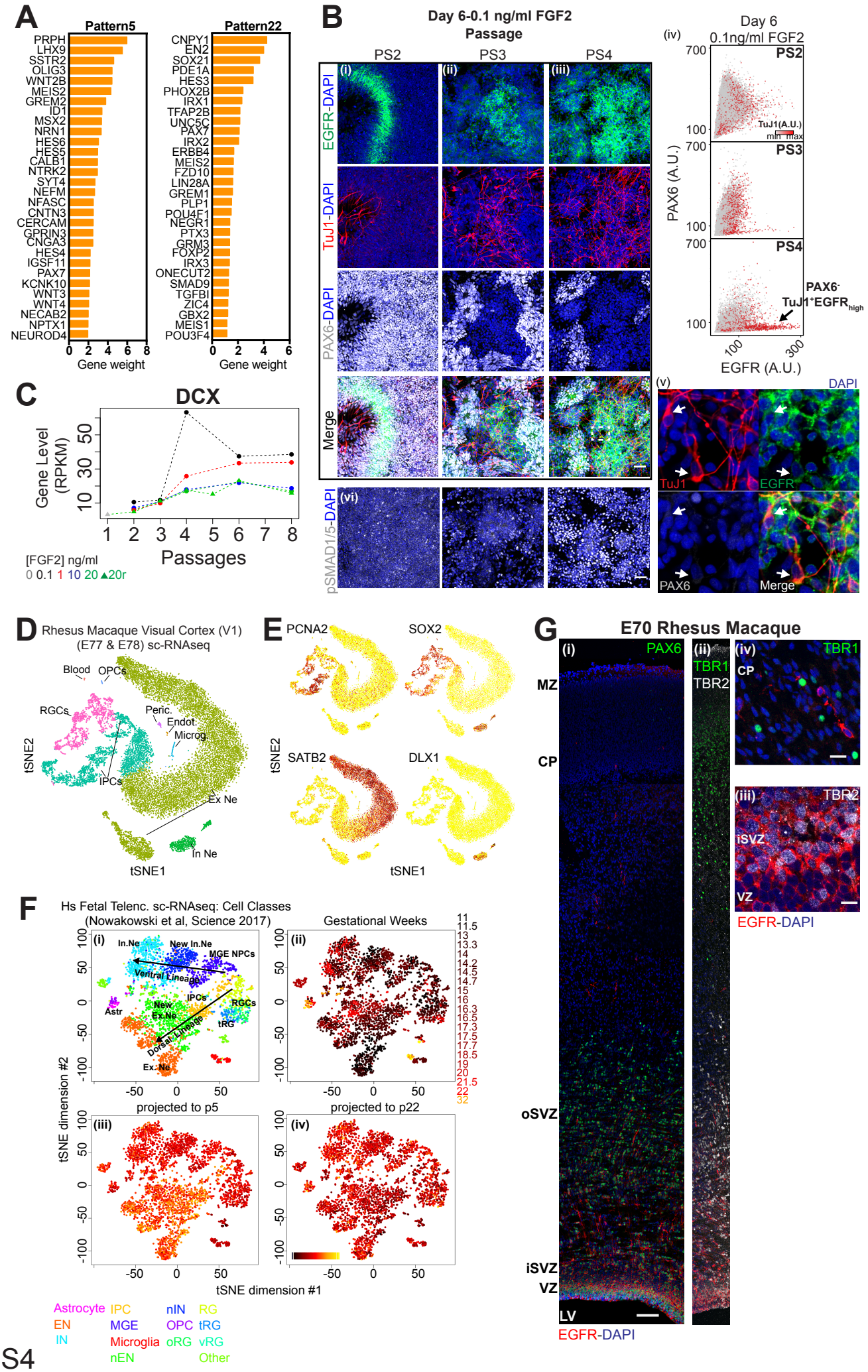
A
Pattern5
PRPH
LHX9
SSTR2
OLIG3
WNT2B
MEIS2
GREM2
ID1
MSX2
NRN1
HES6
HES5
CALB1
NTRK2
SYT4
NEFM
NFASC
CNTN3
CERCAM
GPRIN3
CNGA3
HES4
IGSF11
PAX7
KCNK10
WNT3
WNT4
NECAB2
NPTX1
NEUROD4
0 2 4 6 8
Gene weight
Pattern22
CNPY1
EN2
SOX21
PDE1A
HES3
PHOX2B
IRX1
TFAP2B
UNC5C
PAX7
IRX2
ERBB4
MEIS2
FZD10
LIN28A
GREM1
PLP1
POU4F1
NEGR1
PTX3
GRM3
FOXP2
IRX3
ONECUT2
SMAD9
TGFBI
ZIC4
GBX2
MEIS1
POU3F4
0 2 4 6
Gene weight
B
Day 6-0.1 ng/ml FGF2
Passage
PS2
PS3
PS4
(i)
(ii)
(iii)
EGFR-DAPI
TuJ1-DAPI
PAX6-DAPI
Merge
pSMAD1/5-DAPI
(vi)
(iv)
Day 6
0.1ng/ml FGF2
PS2
PS3
PS4
TuJ1(A.U.)
min max
PAX6 (A.U.)
EGFR (A.U.)
PAX6-
TuJ1+EGFRhigh
(v)
DAPI
TuJ1
EGFR
PAX6
Merge
C
DCX
Gene Level (RPKM)
Passages
[FGF2] ng/ml
0 0.1 1 10 20 ▲20r
D
Rhesus Macaque Visual Cortex (V1)
(E77 & E78) sc-RNAseq
Blood
OPCs
RGCs
Peric.
Endot.
Microg
IPCs
Ex Ne
In Ne
tSNE1
tSNE2
E
PCNA2
SOX2
SATB2
DLX1
tSNE1
tSNE2
F
Hs Fetal Telenc. sc-RNAseq: Cell Classes
(Nowakowski et al, Science 2017)
Gestational Weeks
(i)
In.Ne
New In.Ne
MGE NPCs
Ventral Lineage
IPCs
RGCs
Astr
New Ex.Ne
tRG
Dorsal Lineage
Ex.Ne
(ii)
projected to p5
projected to p22
(iii)
(iv)
tSNE dimension #2
tSNE dimension #1
Astrocyte
EN
IN
IPC
MGE
Microglia
nEN
nIN
OPC
oRG
RG
tRG
vRG
Other
G
E70 Rhesus Macaque
(i)
PAX6
MZ
CP
oSVZ
iSVZ
VZ
LV
(ii)
TBR1
TBR2
(iv)
TBR1
CP
(iii)
TBR2
iSVZ
VZ
EGFR-DAPI

Figure S4

Figure S4. Cortical excitatory neuron fate bias at a specific passage of human NSCs. Related to Figure 3. Cortical neuron differentiation bias of human NSCs varies across passages (**A-C**). (**A**) 30 selected genes among the top 100 most strongly contributing to patterns p5 and p22, shown in Figure 3B. Pattern p5 is enriched in genes expressed during neuronal differentiation and CP formation. Pattern p22 is enriched in genes expressed in neural stem cells. (**B**) (Left) Immuno-fluorescence of hNSCs grown in 0.1 ng/ml FGF2 for 6 days showing expression of EGFR, TuJ1 and PAX6 in PS2 (i), PS3 (ii) and PS4 (iii). Nuclei are stained with DAPI. Scale bar: 50 μm. (iv) Scatter plot of individually segmented EGFR vs PAX6 expressing cells, colored by TuJ1 expression at PS2, PS3 and PS4, from high-throughput image analysis. (v) Higher magnification of the dashed area in (iii-merge) showing EGFR/TuJ1 co-expressing cells, indicated with arrows. (vi) Immuno-fluorescence images of hNSCs grown with 0.1 ng/ml FGF2 for 6 days showing higher induction of pSMAD1/5 in PS4. Nuclei are stained with DAPI. Scale bar: 50 μm. (**C**) Dose-response expression of Doublecortin (DCX) through passages, from H9 derived hNSC RNAseq data. FGF2 doses are indicated. 0 ng/ml FGF2 refers to PS1; 20r refers to PS2-PS8 sample replicates for 20 ng/ml FGF2.
Neurogenic transition states of RGCs in the developing primate cortex (**D-G**). (**D**) t-distributed stochastic neighbor embedding (tSNE) plots colorored by cluster annotation from macaque E77 and E78 Visual Cortex (V1) single cell RNA-seq data. 17161 cells (9193 cells from E77 V1 and 7963 from E78 V1) were analyzed. RGCs: radial glial cells; IPCs: intermediate precursors cells; OPCs: oligodendrocyte progenitor cells; Peric.: pericytes; Endot.: endothelial cells; Microg.: microglia; ExNe: excitatory neurons; InNe: interneurons (**E**) tSNE plots colorored by markers for the major cell clusters: neurons (SATB2); cyclin RGCs and IPCs (PCNA); RGCs and IPCs (SOX2); IPCs (Eomes/TBR2 and NEUROG1) see also Figure 3E; interneurons (DLX1). (**F**) (i-iv) tSNE plots of human fetal telencephalic single-cell RNA-seq data of 3495 cells from (Nowakowski et al., 2017). (i) Depiction of cell classes across dorsal and ventral telencephalic developmental trajectories. Cell clusters nomenclature at the bottom of the figure. (ii) Ages of the donors from which cells derived. (iii and iv) Projections of the human fetal telencephalic single-cell RNA-seq data from (Nowakowski et al., 2017) into p5 (iii) and p22 (iv), colored by magnitude of projection, confirming that p5 is correlated with dorsal post-mitotic neuron signature *in vivo*. MGE NPCs: medial ganglionic eminence neural precursor cells; IPCs: intermediate progenitor cells; RGCs: radial glial cells; EN: excitatory neurons; IN: inhibitory neurons; nEN: new excitatory neurons; nIN: new inhibitory neurons; OPC: oligodendrocyte progenitor cells; oRG: outer radial glial cells; RG: radial glial cells; tRG: truncated radial glial cells; vRG: ventricular radial glial cells. (**G**) (i-iv) Immuno-histochemistry of E70 rhesus macaque dorsal parietal cortex tissues sections for EGFR (red; all panels) together with Pax6 (i), TBR1 and TBR2 (ii), Scale bar: 100 μm; TBR2 in the VZ and iSVZ (iii), Scale bar: 10 μm; TBR1 in CP (iv), Scale bar: 20 μm. Nuclei stained with DAPI. Notice that in (i) sequential tiled images were taken from the same cortical section that then were stitched. Slight tile stitching misalignments and DAPI intensity artifacts were corrected (See Methods).

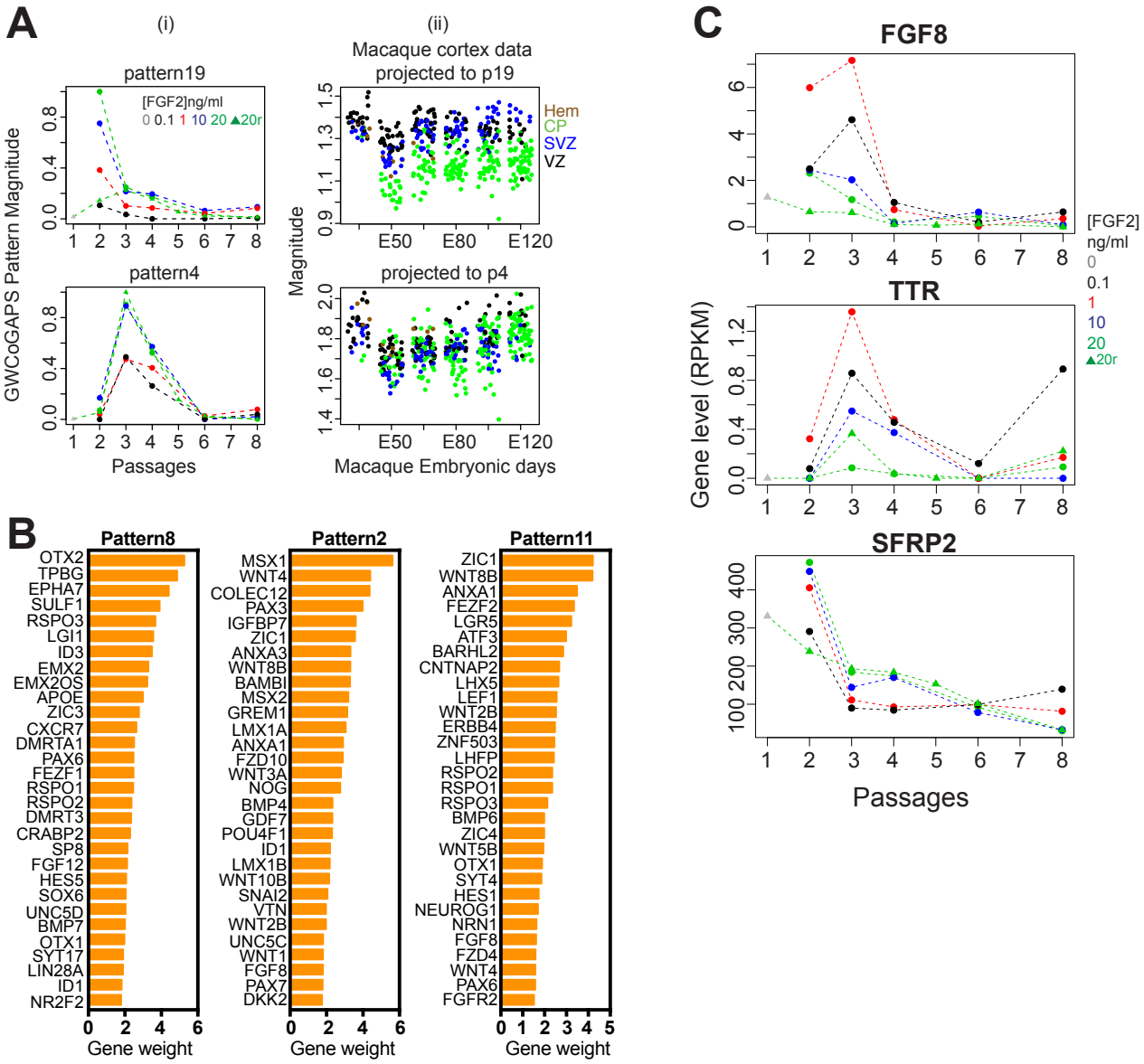
A
(i)
(ii)
pattern19
[FGF2]ng/ml
0 0.1 1 10 20 ▲20r
pattern4
GWCoGAPS Pattern Magnitude
Passages
Macaque cortex data
projected to p19
projected to p4
Magnitude
Hem
CP
SVZ
VZ
E50 E80 E120
Macaque Embryonic days
B
Pattern8
OTX2 TPBG EPHA7 SULF1 RSPO3 LGI1 ID3 EMX2 EMX2OS APOE ZIC3 CXCR7 DMRTA1 PAX6 FEZF1 RSPO1 RSPO2 DMRT3 CRABP2 SP8 FGF12 HES5 SOX6 UNC5D BMP7 OTX1 SYT17 LIN28A ID1 NR2F2
Pattern2
MSX1 WNT4 COLEC12 PAX3 IGFBP7 ZIC1 ANXA3 WNT8B BAMBI MSX2 GREM1 LMX1A ANXA1 FZD10 WNT3A NOG BMP4 GDF7 POU4F1 ID1 LMX1B WNT10B SNAI2 VTN WNT2B UNC5C WNT1 FGF8 PAX7 DKK2
Pattern11
ZIC1 WNT8B ANXA1 FEZF2 LGR5 ATF3 BARHL2 CNTNAP2 LHX5 LEF1 WNT2B ERBB4 ZNF503 LHFP RSPO2 RSPO1 RSPO3 BMP6 ZIC4 WNT5B OTX1 SYT4 HES1 NEUROG1 NRN1 FGF8 FZD4 WNT4 PAX6 FGFR2
Gene weight
C
FGF8
TTR
SFRP2
Gene level (RPKM)
Passages
[FGF2]
ng/ml
0
0.1
1
10
20
▲20r

Figure S5

Figure S5. Cortical organizer identities of early passage human NSCs. Related to Figure 4. (**A**) (i) GWCoGAPS patterns p19 and p4. FGF2 doses are indicated. 0 ng/ml FGF2 refers to PS1; 20r refers to PS2-PS8 sample replicates for 20 ng/ml FGF2. (ii) Projections of microarray data from laser micro-dissected macaque cortex (Bakken et al., 2016) into p19 and p4. CP, cortical plate; SVZ, subventricular zone; VZ, ventricular zone. (**B**) 30 selected genes among the top 100 most strongly contributing to patterns p8, p2 and p11 shown in Figure 4, enriched in genes highly expressed in the cortical hem. (**C**) Dose-response expression of FGF8, TTR, SFRP2 through passages from H9 derived hNSC RNAseq data. FGF2 doses are indicated. 0 ng/ml FGF2 refers to PS1. 20r refers to PS2-PS8 sample replicates for 20 ng/ml FGF2.

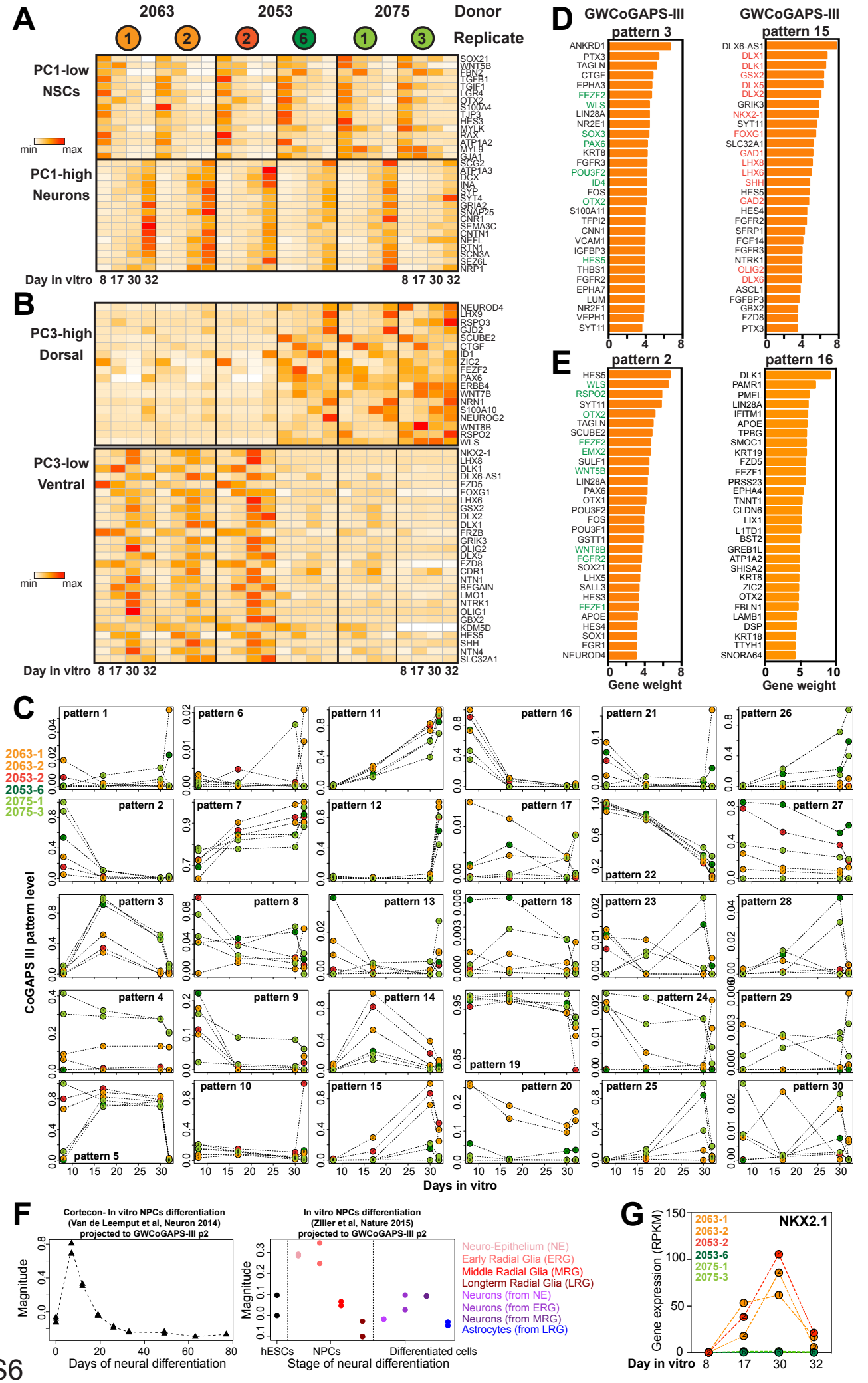
A
2063
2053
2075
Donor
Replicate
PC1-low NSCs
min
max
PC1-high Neurons
Day in vitro 8 17 30 32
8 17 30 32
B
PC3-high Dorsal
PC3-low Ventral
D
GWCoGAPS-III pattern 3
GWCoGAPS-III pattern 15
E
pattern 2
pattern 16
Gene weight
C
2063-1
2063-2
2053-2
2053-6
2075-1
2075-3
CoGAPS III pattern level
Days in vitro
F
Cortecon- In vitro NPCs differentiation (Van de Leemput et al, Neuron 2014) projected to GWCoGAPS-III p2
In vitro NPCs differentiation (Ziller et al, Nature 2015) projected to GWCoGAPS-III p2
Magnitude
Days of neural differentiation
hESCs
NPCs
Differentiated cells
Stage of neural differentiation
Neuro-Epithelium (NE)
Early Radial Glia (ERG)
Middle Radial Glia (MRG)
Longterm Radial Glia (LRG)
Neurons (from NE)
Neurons (from ERG)
Neurons (from MRG)
Astrocytes (from LRG)
G
NKX2.1
Gene expression (RPKM)
Day in vitro 8 17 30 32

Figure S6

Figure S6. Human NSC line variation in organizer states results in divergent neuronal fate trajectories. Related to Figure 5. (**A**) Heatmap showing expression levels of NSC - and neuron-related genes that are highly represented at the extremes of PC1, shown in Figure 5Bi, demonstrating the transition from neural precursors to neurons in all 6 hiPSC lines. (**B**) Heatmap showing expression levels of dorsal and ventral fate specification-related genes that are highly represented at the extremes of PC3, shown in Figure 5Bii, demonstrating distinct regional bias of each group of cell lines. (**C**) 30 patterns defined by GWCoGAPS of the 6 hiPSC lines data set, indicated as GWCoGAPS-III p1-p30. (**D**) 30 selected genes among the top 100 most strongly contributing to the GWCoGAPS-III p3 and p15 shown in Figure 5C. Well-known dorsal (green) and ventral (red) fate specification genes are highlighted. (**E**) 30 selected genes among top 100 most strongly contributing to the GWCoGAPS-III p2 and p16 shown in Figure 5D. Well-known genes of the cortical hem (in green) are highly expressed at day 8 in the lines with dorsal lineage bias. (**F**) Projection of public sequencing data of differentiating cortical neurons derived from hiPSCs (van de Leemput et al., 2014; Ziller et al., 2015) into the hem-associated GWCoGAPS-III p2. The data confirm the emergence of early organizers in hNSCs *in vitro* generated in other labs with other protocols. NSC types classified in (Edri et al., 2015; Ziller et al., 2015) are on the right. (**G**) Expression of the ventral gene NKX2.1 across the differentiation of the 6 iPSC lines. The marker is expressed at late time points by the ventral biased hNSC lines.